MINISTRY OF EDUCATION AND TRAINING

VIETNAM ACADEMY OF AND TECHNOLOGY

GRADUATE UNIVERSITY OF SCIENCE AND TECHNOLOGY

Doan Tien Dat

FABRICATION OF NANOSTRUCTURED ELECTRODES FOR ORGANIC PHOTOVOLTAIC DEVICES AND ELECTROCHEMICAL SENSORS

SUMMARY OF DISSERTATION ON SCIENCES OF MATTER

Major: Organic Chemistry

Code: 9.44.01.14

HA NOI - 2025

The dissertation is completed at: Graduate University of Science and Technology, Vietnam Academy Science and Technology

Supervisors:

1: Supervisor 1: Assoc. Prof. Hoang Mai Ha

2: Supervisor 2: Dr. Pham Thi Hai Yen

Referee 1: .....

Referee 2: .....

Referee 3: .....

The dissertation is examined by Examination Board of Graduate University of Science and Technology, Vietnam Academy of Science and Technology at…….. (time, date……)

The dissertation can be found at:

1. Graduate University of Science and Technology Library

2. National Library of Vietnam

INTRODUCTION

In the context of an increasingly global emphasis on sustainable energy solutions and a green living environment, the technology of organic solar cells (OPV) and electrochemical sensors is garnering significant research attention due to its strong development potential. OPVs, with their advantages of being lightweight, flexible, and low-cost, are expected to replace traditional silicon-based solar cell technologies. The performance and durability of OPV devices heavily depend on the quality of electrodes, with indium tin oxide (ITO) electrodes often utilized. However, ITO electrodes have drawbacks, such as mechanical brittleness and the increasing scarcity of indium supply. Consequently, scientists are exploring the development of flexible, cost-effective, and easily processable electrodes made from materials like graphene, carbon nanotubes, silver nanowires, and conductive polymers. Initial efforts have demonstrated the potential for producing electrodes with high transparency and good conductivity. Nevertheless, durability and surface roughness remain, limiting their applications in optoelectronic devices.

Moreover, the urgent need for environmental quality monitoring necessitates the development of highly sensitive and selective electrochemical sensors. These sensors, with their ability to detect various pollutants at low concentrations, high mobility, and reasonable operating costs, play a crucial role in building an efficient environmental monitoring system. The performance of electrochemical sensors depends significantly on the quality of the working electrode. The electrode not only acts as a catalyst for electrochemical reactions but also serves as a site for analyte accumulation and electron transfer. Therefore, the design and fabrication of nanostructured electrodes with large surface area and high electrical conductivity is one of the key research directions aimed at enhancing the sensitivity and selectivity of sensors.

To address the need for nanostructured electrodes made from advanced materials that meet requirements for transparency, electrical conductivity, active surface area, and applicability in optoelectronic devices and electrochemical sensors, a thesis titled "Fabrication of nanostructured electrodes for organic photovoltaic devices and electrochemical sensors" has been proposed.

Research objectives of the thesis:

The thesis aims to:

- ❖ Fabricate flexible, transparent nanostructured electrodes with high conductivity and transmittance for applications in optoelectronic components.
- ❖ Fabricate nanostructured electrodes with large active surface area and high charge transfer capacity for applications in electrochemical sensors to detect pollutants in water with high sensitivity.

Main research contents:

- ❖ Content 1: Synthesis and modification of some nanomaterials suitable for manufacturing electrodes for application in organic solar cell components and electrochemical sensors.
- ❖ Content 2: Fabrication of flexible, transparent nanostructured photolithographic electrodes for application in organic solar cell components.
- ❖ Content 3: Fabrication of nanostructured electrodes for application in electrochemical sensors to detect heavy metal ions and antibiotic residues in water.

CHAPTER 1: OVERVIEW

In the Overview section, the dissertation has:

- Presented a comprehensive summary of various nanostructured materials applied in the fabrication of optoelectronic devices and electrochemical sensors.
- Provided an overview of the fabrication methods and research progress on the use of nanostructured electrodes in optoelectronic devices and electrochemical sensors, detailing both international and domestic research efforts in this field.
- Additionally, the Overview section highlights the limitations of previously published studies and emphasizes the advantages of the research conducted in the dissertation

CHAPTER 2. EXPERIMENT AND METHODOLOGY

In the Experimental section, the dissertation has:

- Presented the synthesis methods for various nanostructured materials, including AgNW, GO, PEDOT:PSS, oxidized CNT, CuBTC MOF, and bimetallic FeMg-BDC MOF.
- Elaborated on the fabrication methods for photolithographic electrodes and organic solar cell devices.
- Detailed the methods for electrode fabrication and modification in electrochemical sensors.
- Highlighted the characterization techniques for the properties of materials, electrodes, as well as the characteristics of organic solar cell devices and electrochemical sensors after fabrication.

CHAPTER 3. RESULTS AND DISCUSSION

3.1. RESULTS OF MATERIAL SYNTHESIS

3.1.1. Results of silver nanowires synthesis

Silver nanowires (AgNW) were successfully synthesized using the polyol method. The synthesized AgNW have a length ranging from 10-15 µm and an average diameter of approximately 30-40 nm (Fig 3.1).

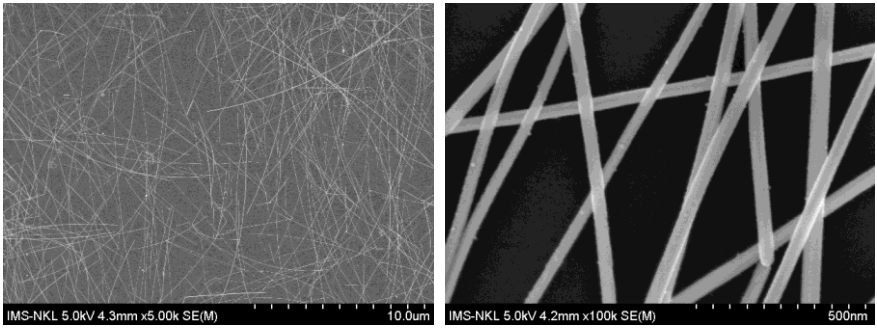

Fig 3.1. FESEM image of silver nanowires

3.1.2. Results of graphene oxide synthesis

Graphene oxide was synthesized by the Hummer method. The synthesized graphene oxide is a thin, transparent layer that can disperse well in water, suitable for the fabrication of nanostructured electrodes (Fig 3.2).

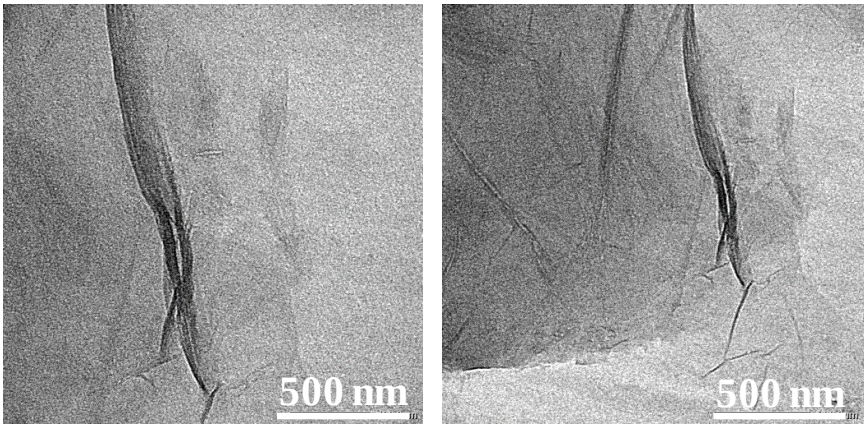

Fig 3.2. TEM image of graphene oxide

3.1.3. Results of PEDOT:PSS synthesis

After synthesis, PEDOT:PSS was dispersed in water at a

concentration of 2%. The solution exhibits high stability and is stored at 4 °C. Figure 3.3 shows the SEM image of the synthesized PEDOT:PSS sample. The formation of particles with sizes ranging from a few nanometers to several tens of nanometers enables PEDOT:PSS to maintain stable dispersion in water.

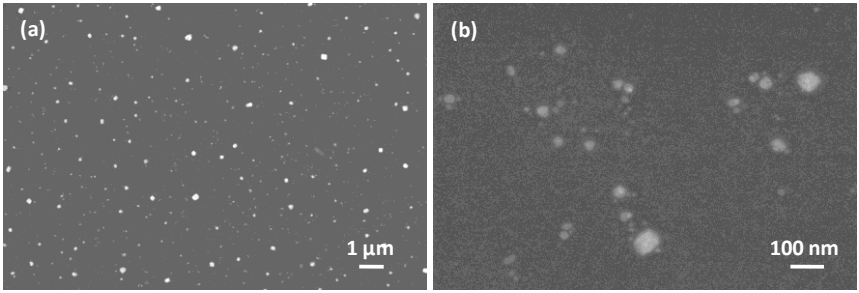

Fig 3.3. FESEM image of PEDOT:PSS

3.1.4. CNT oxidation results

Based on the FT-IR analysis results, it can be seen that the oxygen-containing functional groups have been successfully attached to the CNT surface. After oxidation, the CNT still retains the tubular structure (Figure 3.4) and can disperse well in water.

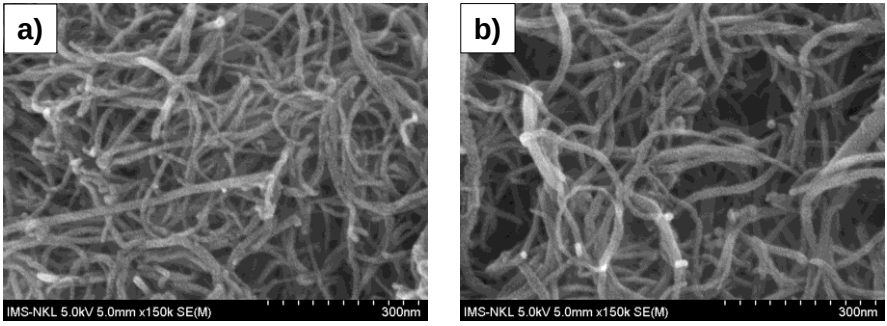

Fig 3.4. SEM images of (a) original CNTs and (b) oxidized CNTs

3.1.5. Results of bimetallic MOF FeMg-BDC synthesis

SEM images, EDS spectra, and XRD patterns confirm the successful

synthesis of the bimetallic organic framework FeMg-BDC. The bimetallic FeMg-BDC MOF crystals exhibit a rice grain-like shape, with Fe and Mg metal centers evenly distributed within the structure. Furthermore, BET surface area measurements indicate that the bimetallic FeMg-BDC MOF has a superior BET active surface area compared to the monometallic FeBDC and MgBDC MOFs.

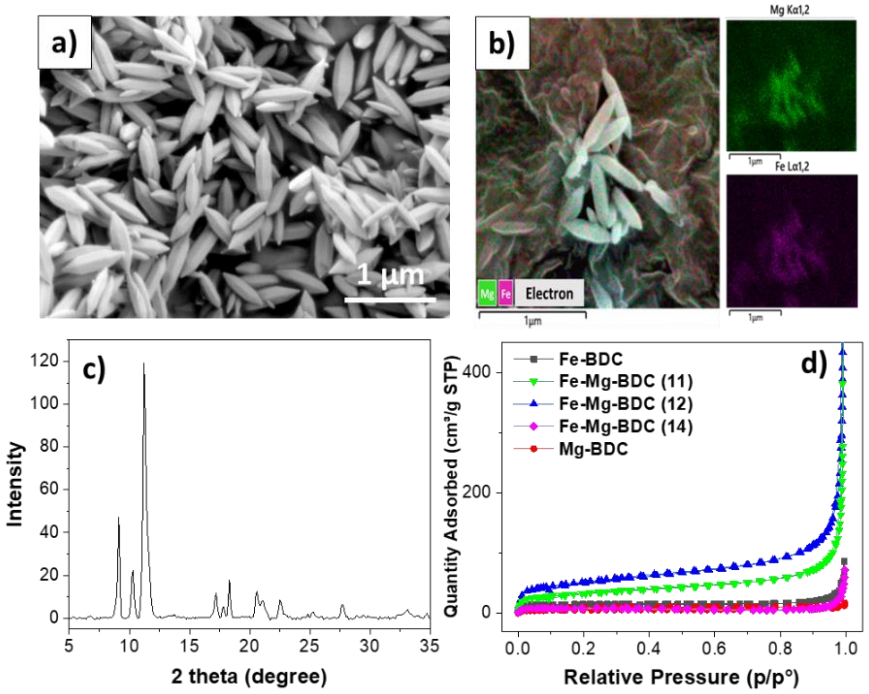

Fig 3.5. SEM image, EDS mapping spectrum, XRD pattern of FeMg-BDC (1/2) bimetallic MOF, and adsorption and desorption isotherms of MOF material samples

3.1.6. Results of CuBTC-CNT synthesis

SEM images, XRD patterns, and XPS spectra confirmed that MOF CuBTC was successfully synthesized. After synthesis, CuBTC was evenly mixed with CNT to form CuBTC-CNT composite material.

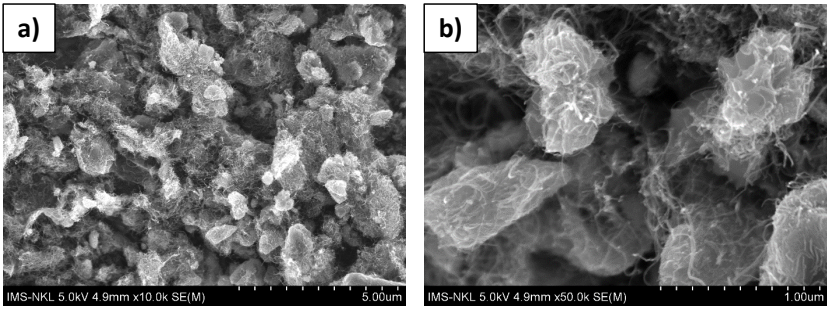

Fig 3.6. SEM image of CuBTC-CNT material

3.2. RESULTS OF FABRICATION OF TRANSPARENT FLEXIBLE ELECTRODES AND ORGANIC PHOTOVOLTAICS DEVICES

3.2.1. Surface morphology of PET/x-PVCn/AgNW$_{press}$ patterned electrodes

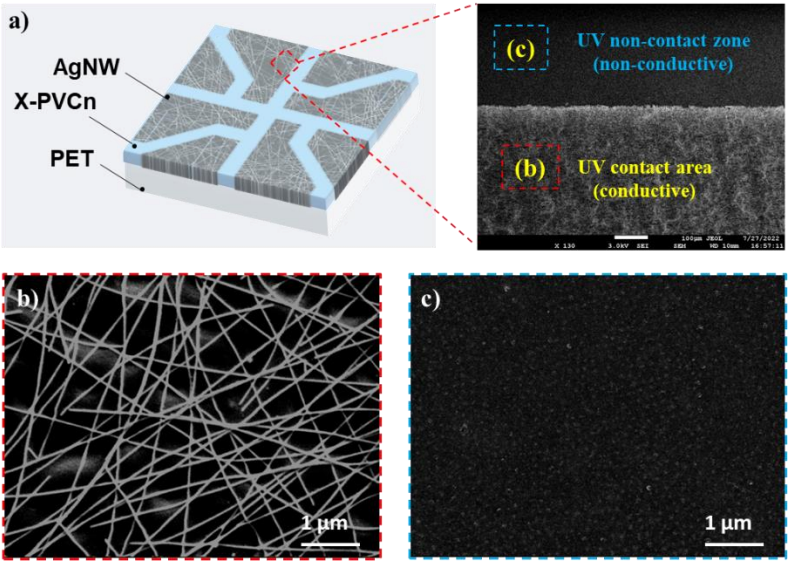

Fig 3.7. Structure of the PET/x-PVCn/AgNW$_{press}$ patterned electrodes after fabrication and SEM images of the UV-irradiated and non-UV-irradiated areas on the electrode surface

SEM images reveal that the patterned electrode PET/x-PVCn/AgNW$_{press}$ was successfully fabricated. The electrodes exhibit high

resolution, showing clear boundaries between regions exposed to UV radiation and regions not exposed (Fig 3.7a). In UV-exposed regions, the PVCn layer is cured, effectively protecting the AgNW from being washed away by THF (Fig 3.7b). Meanwhile, in regions not exposed to UV radiation, the uncured PVCn layer is washed away along with the AgNW layer above it, resulting in a non-conductive area (Figure 3.7c).

3.2.2. Properties of OPV devices using PET/x-PVCn/AgNW$_{press}$ electrodes

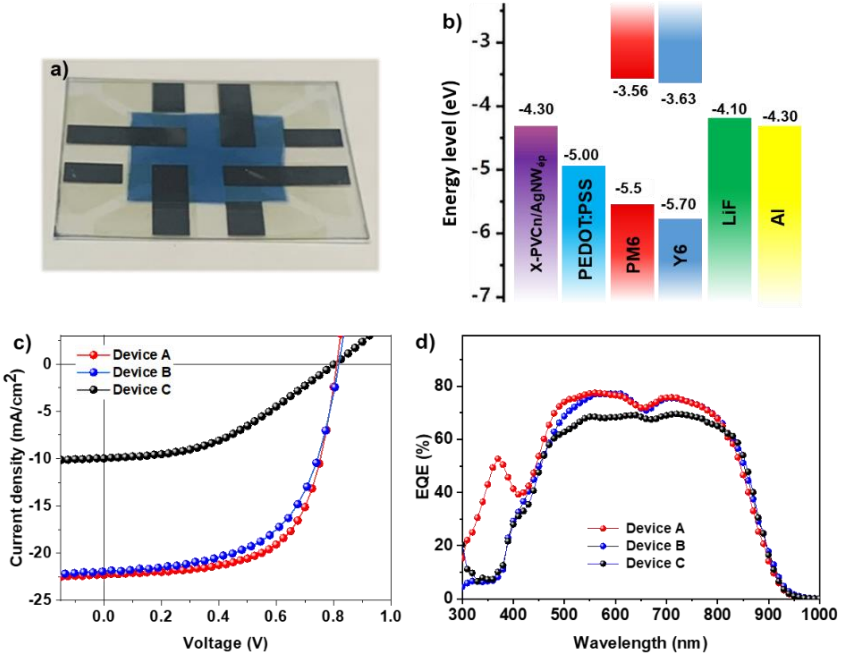

Fig 3.8. a) Structure of PM6 and Y6 molecules used as active layers in the device, b) Energy band structure of the layers in the OPV device, c) J-V characteristic curve, and d) EQE quantum efficiency spectrum of the device

The organic solar cell (OPV) device utilizing the photolithographic electrode PET/x-PVCn/AgNWép (Device B) was fabricated following the structure illustrated in Figure 3.8a, with PM6 and Y6 used as the active layer

materials (Figure 3.8b). OPV devices employing PET/ITO electrodes (Device A) and PET/AgNW electrodes (Device C) were also fabricated simultaneously as reference devices. The J-V characteristics of these devices are shown in Figure 3.8c. Device C, which uses AgNW electrodes, exhibited the lowest photovoltaic efficiency of 3.46%. This result can be attributed to the AgNW electrode's poor electrical conductivity and transmittance. Additionally, its high surface roughness compromised the contact quality between the electrode and the active layer.

Meanwhile, the device employing the photolithographic electrode PET/x-PVCn/AgNWép (Device B) achieved a power conversion efficiency (PCE) of 11.24%, comparable to the PCE of the device using ITO electrodes on a PET substrate (11.54%). The EQE (External Quantum Efficiency) spectra measurements further corroborated the energy conversion efficiency results of the devices (Figure 3.8d).

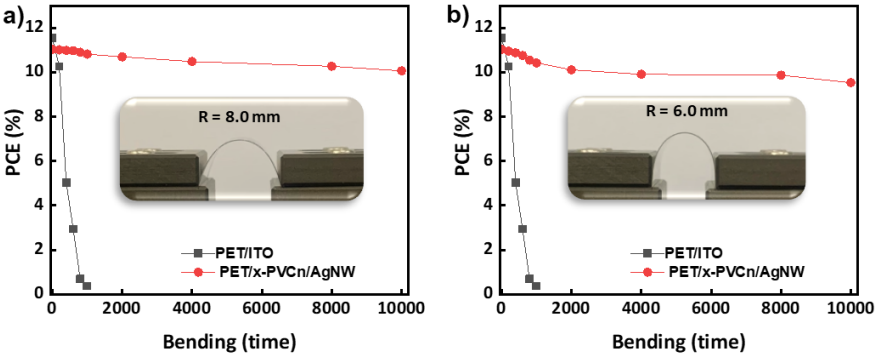

Fig 3.9. Change in PCE value of OPV device

Additionally, the device utilizing the photolithographic electrode PET/x-PVCn/AgNWép demonstrated superior bending durability compared to the device using an ITO electrode (Figure 3.9). Device A exhibited a significant reduction in PCE and became completely damaged after 1,000 bending cycles with a radius of 8 mm. In contrast, Device B showed only an

8.9% reduction in PCE after 10,000 bending cycles at the same radius (Figure 3.9a). When bent at a radius of 6 mm, Device A failed after approximately 500 cycles. Device B, however, retained 86.3% of its initial PCE even after 10,000 cycles. These results highlight the high bending durability of the OPV device employing the photolithographic electrode PET/x-PVCn/AgNWép.

3.3. RESULTS OF FABRICATION OF WORKING ELECTRODE FOR APPLICATION IN ELECTROCHEMICAL SENSORS

3.3.1. Electrodes in electrochemical sensors for antibiotic detection

3.3.1.1. rCNT/GCE electrode for analysis of ENR

+ Electrochemical properties of rCNT/GCE electrode:

The electrochemical properties of the electrodes were studied by the impedance spectroscopy (EIS) method and the cyclic voltammetry (CV) method from 0.8 to -0.4 V. The results showed that the rCNT/GCE electrode has superior charge transfer capacity and surface active area compared to the bare GCE electrode as well as other modified electrodes (Table 3.1). Therefore, the rCNT/GCE electrode is expected to be suitable for electrochemical sensors to detect ENR with good efficiency.

Bảng 3.1. Electrochemical impedance and electrochemically active surface area of electrodes

Electrode	R_{ct} (Ω)	EASA (cm^2)
GCE	350	0,07
CNT/GCE	27	0,075
oCNT/GCE	50,3	0,08
rCNT/GCE	23,7	0,131

+ Electrochemical signal of ENR on rCNT/GCE electrode

The electrochemical signals of ENR on the electrodes were evaluated by CV measurements in PBS solution (pH=7) containing 10 µM ENR at a fixed scan rate of 0.3 V/s. The obtained data showed that the ENR reaction was an irreversible oxidation process, since only the oxidation signal of ENR (at 0.85 V) was obtained without any reduction peak in the reverse scan direction. This result indicated that the fabricated electrode was applicable for the determination of ENR. For further studies, a linear voltammetric (LSV) method with a scan potential range of 0.3 to 1.3 V was used to record the electrochemical signals of ENR.

+ Effect of oCNT concentration on the electrochemical signal of ENR

To investigate the effect of oCNT concentration on the ENR analysis ability of rCNT/GCE electrode, electrodes were fabricated using solutions with different oCNT concentrations (0.005%, 0.01%, 0.02%, 0.03% and 0.04%). The results showed that the rCNT/GCE electrode fabricated with oCNT concentration of 0.02% gave the clearest ENR signal. Therefore, oCNT solution with a concentration of 0.02% was chosen to fabricate electrodes for subsequent electrochemical analysis.

+ Optimize ENR analysis conditions

Factors such as electrolyte solution, pH of electrolyte solution and accumulation time were investigated. The results showed that the suitable electrolyte solution was PBS buffer solution with pH = 8, the suitable accumulation time was 120 s with high ENR concentration level and 600 s with low ENR concentration level.

+ Calibration curve for ENR detection

The calibration curve correlating the electrochemical signal with various ENR concentrations (ranging from 0.05 to 1.5 µM) was constructed using the LSV method in a 0.1 M PBS solution (pH=8) (Figure 3.10). The analytical conditions included a scan rate of 0.3 V/s and an accumulation time of 120 seconds. The obtained results show that the peak current increases linearly with ENR concentration. Figure 3.10 illustrates the linear

relationship between the peak current values and different ENR concentrations, expressed by the linear regression equation Ip(µA) = 10.269(µM) + 0.0493 with a correlation coefficient R^2 = 0.9994.

Additionally, a calibration curve was constructed for lower ENR concentrations, ranging from 0.005 to 0.05 µM, using an accumulation time of 600 seconds (Fig 3.10b). The relationship between peak current and ENR concentration is described by the linear regression equation Ip(µA) = 99.423(µM) + 0.0412, with a determination coefficient R^2 = 0.9991. The limit of detection (LOD) was calculated to be 0.002 µM within the concentration range of 0.005–0.05 µM. Notably, this LOD value is significantly lower than the permissible ENR concentration in milk and muscle tissue as regulated by the European Union (100 ppb ~ 0.27 µM).

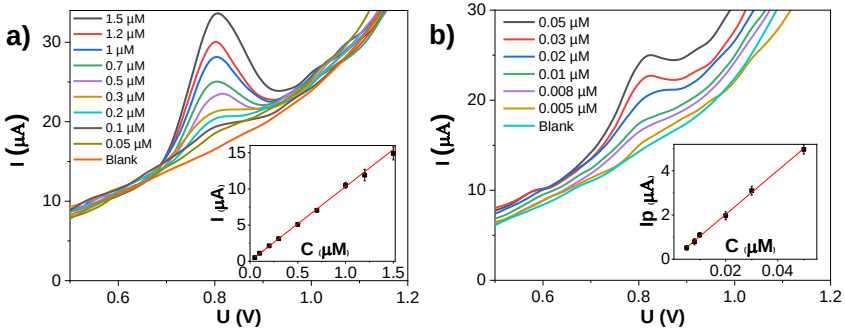

Fig 3.10. Electrochemical signals of ENR at different concentrations with accumulation times of 120s (a) and 600s (b).

+ Detection of ENR in real samples

The ENR concentration in shrimp meat samples was determined by the standard addition method. The calculated recovery was 96.3%, indicating the high accuracy of the sensor. This result demonstrates the effectiveness of the electrochemical ENR analysis method using rCNT/GCE electrode, thereby demonstrating the potential of this method in real sample analysis.

3.3.1.2. CuBTC-CNT@CPE electrode for analysis of ENR

+ Electrochemical properties of CuBTC-CNT@CPE electrode

Electrochemical impedance spectroscopy was performed on bare CPE and CNT@CPE, CuBTC@CPE, and CuBTC-CNT@CPE electrodes. Based on EIS analysis, the Rct value calculated for bare CPE was found to be approximately 1100 Ω, while the value for CuBTC-modified CPE increased to nearly 2000 Ω. These data indicate that the electron transfer capability on the CuBTC@CPE surface is lower than that of the unmodified CPE electrode. However, when CuBTC was combined with CNT, the Rct value of CuBTC-CNT@CPE was approximately 577 Ω. This value decreased significantly compared to bare CPE. This is due to the presence of CNT, a good conductor, which improves the charge transfer capability on the electrode surface. Thus, the mutual effect of CuBTC materials with porous properties, the existence of COOH functional groups and CNT with good electrical conductivity, CuBTC-CNT@CPE electrode has great potential in increasing the efficiency of ENR analysis.

+ Electrochemical signal of ENR on rCNT/GCE electrode

To investigate the electrochemical properties of ENR on the electrodes, CV measurements were performed in PBS solution (pH = 7) containing 200 μM ENR at a fixed scan rate of 0.3 V/s from 0.0 to 1.2 V (Fig. 3.35a). The obtained data showed the oxidation of ENR on the electrodes. Specifically, the oxidation signal of ENR was observed at around 0.9 V, while no reduction peak was seen in the reverse scan direction. Significantly, the ENR oxidation signal on the CuBTC-modified electrodes increased, and the CuBTC-CNT@CPE electrode showed the highest signal. The results confirmed the ability of the CuBTC framework to enrich ENR through adsorption and the ability of CNT to enhance the charge transfer rate on the electrode surface.

+ Effect of CNT concentration on the electrochemical signal of ENR

The effect of CNT content in the material composition on the ENR oxidation signal was evaluated by varying the CNT content in the electrode composition from 1 to 4%. The electrochemical signals showed that the peak current intensity increased as the CNT content increased up to 3%. The peak current decreased as the CNT content further increased up to 4%. Therefore, the composite material containing 3% CNT was used to fabricate the electrode for further experiments.

+ Optimize ENR analysis conditions

Factors such as electrolyte solution, pH of electrolyte solution and accumulation time were investigated. The results showed that the suitable electrolyte solution was PBS buffer solution with pH = 7, accumulation time 0 s and 90 s were selected for ENR concentrations higher than 1 μM and 0.1 μM, while accumulation time 300 s was used for solutions with lower concentrations.

+ Calibration curve for ENR detection

The applicability of CuBTC-CNT@CPE for the quantification of ENR was investigated by constructing calibration curves correlating the peak currents of the SWV signal with the concentrations of standard ENR solutions. SWV signals for three concentration ranges with three different accumulation times—0 seconds, 90 seconds, and 300 seconds (1–12 μM, 0.1–1.0 μM, and 0.01–0.20 μM)—are presented in Figure 3.38a, c, and d. The results indicate a gradual increase in the peak oxidation current response with increasing ENR concentrations. For the concentration range of 1 to 12 μM, a clear linear relationship was observed between the peak oxidation current values obtained without accumulation and the ENR concentrations. At an accumulation time of 0 seconds, the relationship between ENR concentration and the electrochemical signal is described by the linear regression equation $y=0.783x-0.016y = 0.783x - 0.016$, with a determination coefficient $R^2=0.9992$.

For concentrations ranging from 0.1 to 1 μM with an accumulation time of 90 seconds, the correlation between the peak current and ENR concentration is expressed by the linear regression equation $y=13.263x-0.23y = 13.263x - 0.23$, with a high determination coefficient $R^2=0.9995$ (Figure 3.38d).

Additionally, for lower concentrations (0.01 to 0.2 μM), the relationship between the peak current obtained after an accumulation time of 300 seconds and ENR concentration is well described by the linear regression equation $y=46.315x-0.036y = 46.315x - 0.036$, with $R^2=0.9998$. Within this range, the limit of detection (LOD) for the sensor in ENR analysis was determined to be 0.003 μM.

+Detection of ENR in real samples

CuBTC-CNT@CPE was utilized to evaluate ENR concentrations in various real-world samples, including tap water, surface water from West Lake, and seawater. The analysis results were obtained using the standard addition method (Table 3.3). For tap water and surface water from West Lake at ENR concentrations of 0.2 μM and 0.3 μM, the recovery rates ranged from 99.0% to 101.5%. In seawater samples with an ENR concentration of 0.1 μM, the recovery rate was 99.0%. These values are consistent with AOAC standards at the measured concentrations. The relative standard deviation (RSD) values were below 5%, indicating high reliability of the analysis. These findings underscore the accuracy and efficacy of the electrochemical method utilizing CuBTC-CNT/CPE electrodes for ENR detection in real sample analysis.

3.3.2. Electrodes in electrochemical sensors for detecting heavy metals

+ Selecting suitable electrodes for Pb^{2+} detection

Table 3.2. Electrochemical impedance and electrochemically active surface area of electrodes

Electrode	R_{ct} (Ω)	EASA (cm^2)	I_p (μA)
GCE	180	0.07	0.05
Fe-BDC	229	0.055	0.11
Mg-BDC	398	0.059	0.07
FeMg-BDC	70	0.12	0.88
GO/FeMg-BDC	413	0.046	0.91
rGO/FeMg-BDC	55.7	0.14	1.08

The electrochemical properties of the electrodes were investigated by EIS and CV methods in the range of 0.8 to -0.4 V. The results showed that the rGO/FeMg-BDC electrode had superior charge transfer capacity and surface active area compared to the bare GCE electrode as well as other modified electrodes (Table 3.2).

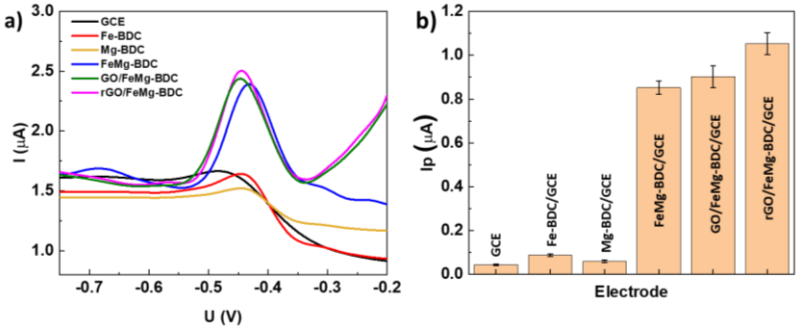

Figure 3.11. (a) SWASV signal and (b) bar graph showing the peak current at different electrodes in 0.1 M KCl buffer solution (KBS) pH = 3 containing 1 μg/L Pb^{2+} and accumulation time of 120 s

With such electrochemical properties, the maximum SWASV current intensity of Pb^{2+} on the rGO/FeMg-BDC electrode was also clear and highest. In addition, the rGO layer on the surface of the rGO/FeMg-BDC

electrode also had the effect of covering and protecting the MOF material layer, making the electrode more durable during the analysis process.

+ Optimize analysis conditions

Factors such as electrolyte solution, pH of electrolyte solution, enrichment electrolysis potential and electrolysis time were investigated. The results showed that the suitable electrolyte solution was KCl-HC buffer solution with pH = 3, the suitable enrichment electrolysis time was 120s with an electrolysis potential of -0.8V.

+ Calibration curve for Pb^{2+} detection

The calibration curves for the Pb2+ detection with varying concentrations of Pb^{2+} (ranging from 0.01 to 50 µg/L) solution was constructed by recording SWASV in 0.1 M KCl – HCl at pH = 3 with deposition potential at -0.8 V during 120 s (Fig. 12a,c). Fig 3.12b,d display the linear relationship between the peak oxidation current values and the Pb2+ concentration, at 2 concentration ranges. From 0.01 µg/L to 0.5 µg/L, the linear regression equation between signal and Pb2+ concentration is Ip (µA) = 1.7127 (µg/L) + 0.0148 with the coefficient of determination R2 = 0.9994. Meanwhile, with concentrations from 0.5 to 50 µg/L, the corresponding regression equation is Ip (µA) = 0.16574 (µg/L) + 0.8334 with a high coefficient of determination R^2 = 0.9991.

This result is attributed to the fact that as the concentration of Pb^{2+} increases, the active sites on the electrode surface become saturated gradually. This saturation makes Pb^{2+} adsorption more difficult on the electrode surface, slowing electrochemical signal growth.5 The limit of detection (LOD) for Pb^{2+} was determined using the standard deviation (σ) of the calibration curve within the 0.01–0.5 µg/L concentration range and its slope (b). The calculated LOD value was 0.009 µg/L, significantly lower than the permissible limit of 10 µg/L set by the World Health Organization (WHO) for lead in drinking water.

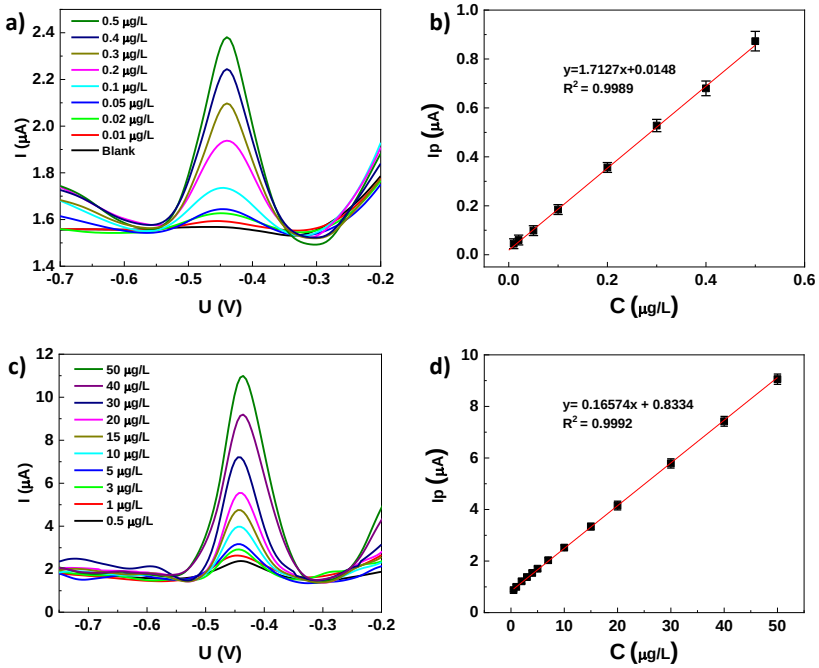

Figure 3.12. SWASV signals of the electrochemical sensor based on rGO/FeMg-BDC electrode for Pb^{2+} determination and linear relationship between peak current and Pb^{2+} concentration. (a, b) from 0.01 – 0.5 µg/L; (c, d) from 0.5 to 50 µg/L.

+ Determination of Pb^{2+} in real samples

The applicability of the fabricated electrode for Pb^{2+} detection in real samples was assessed using the standard addition method. The relative standard deviation (RSD) was determined by measuring each sample three times. Pb^{2+} concentrations have values of 3.29 µg/L, 0.20 µg/L, and 2.65 µg/L for Ha Long seawater, Red River water, and West Lake water samples, respectively. These results are similar to those obtained via inductively coupled plasma mass spectrometry (ICP-MS), demonstrating good accuracy of the rGO/Fe-Mg-BDC/GCE sensor for Pb^{2+} detection in real samples.

CHAPTER IV. CONCLUSION

➢ 1. Synthesis of materials: The researcher has successfully synthesized and modified a number of nanostructured materials containing organic functional groups such as graphene oxide, oxidized CNT, PEDOT:PSS conducting polymer, CuBTC/CNT metal-organic framework composite, FeMg-BDC bimetallic metal-organic framework, and silver nanowires. These materials have good charge transfer properties and are suitable for fabricating nanostructured electrodes.

➢ 2. Fabrication of nanostructured electrodes for application in OPV devices:

- Successfully fabricated a transparent flexible nanostructured electrode on a polyethylene terephthalate (PET/x-PVCn/$AgNW_{press}$) substrate. The electrode has high conductivity and transmittance, low surface roughness, and sharp resolution.

- The PET/x-PVCn/$AgNW_{press}$ electrode was successfully used to fabricate an OPV device with an energy conversion efficiency of 11.24%, equivalent to that of the component using commercial ITO electrodes. In addition, the OPV device using the PET/x-PVCn/$AgNW_{press}$ electrode also has high bending strength when maintaining the energy conversion efficiency after 10,000 bending times.

➢ 3. Fabrication of nanostructured electrodes for electrochemical sensors:

- Nanostructured electrodes were fabricated and applied in electrochemical sensors for analysis of ENR antibiotic residues and Pb^{2+} ions.

- Antibiotic analysis: rCNT/GCE and CuBTC-CNT@CPE electrodes have been fabricated and applied to analyze enrofloxacin. These sensors are highly sensitive, with LODs of 0.002 µM and 0.003 µM, respectively.

- Heavy metal ions analysis: The rGO/FeMg electrode was fabricated and applied for Pb^{2+} analysis. This sensor is highly sensitive, with LODs of 9 ng/L, and is capable of accurately analyzing Pb2+ ions in surface water samples.

LIST OF PUBLICATIONS RELATED TO THE DISSERTATION

1. Fabrication and Application of Functionalized Carbon Nanotubes for Highly Sensitive and Selective Sensing of Enrofloxacin. Vietnam Journal of Chemistry, 2024, 62, S1, 76-85. **Tien Dat Doan**, Thi Hai Yen Pham, Nhung Hac Thi, Ho Thi Oanh, Mai Ha Hoang

2. A Novel Electrochemical Sensor Based On CuBTC Metal-Organic Framework Decorated With Carbon Nanotube For Highly Sensitive Detection Of Enrofloxacin In Water Samples. Journal of Applied Electrochemistry, 2025 55, 189–202. **Tien Dat Doan**, Thi Thao Tran, Thu Hang Nguyen, Manh B. Nguyen, Hoang Anh Nguyen, Ba Viet Anh Pham, Thi Thu Ha Vu, Thi Kim Thuong Nguyen, Mai Ha Hoang, Thi Hai Yen Pham

3. A highly sensitive electrochemical sensor for the detection of lead(II) ions utilizing rice-shaped bimetallic MOFs incorporated reduced graphene oxide. RSC Advances, 2025, 15, 5356. **Tien Dat Doan**, Thi Hai Yen Pham, Dinh Dung Luong, Ho Thi Oanh, Thu Thao Le, Ha Tran Nguyen, Thi Kim Dung Hoang, Mai Ha Hoang

4. Fabrication of Transparent Flexible Electrodes on Polyethylene Terephthalate Substrate with High Conductivity, High Transmittance, and Excellent Stability. Vietnam Journal of Science, Technology and Engineering, 2023, 65(3), 27-31. **Tien Dat Doan**, Nhung Hac Thi, Ho Thi Oanh, Tuyen Nguyen Duc, Mai Ha Hoang

5. Fabrication of Nanostructured Hybrid Electrodes based on Silver Nanowires and Graphene Oxide for Electrochemical Sensor to Detect Lead Ions. International scientific conference on current prospects and challenges in chemistry, 2023. **Tien Dat Doan**, Hoang Van Toan, Nguyen Duc Tuyen, Thi Hai Yen Pham, Mai Ha Hoang.

6. Highly Sensitive Electrochemical Sensor Utilizing CuBDC-NH2 Metal-Organic Framework Combined with Reduced Graphene Oxide for Detecting Pb(II) in Water. Hội thảo hướng môi trường và năng lượng. 2025. **Tien Dat Doan**, Dinh Dung Luong, Tuyen Nguyen Duc, Yen Thi Hai Pham, Mai Ha Hoang